FEBS Letters 588 (2014) 2957–2963

FEBS Letters

journal homepage: www.FEBSLetters.org

miR-140-5p suppresses BMP2-mediated osteogenesis in undifferentiated human mesenchymal stem cells

Supyong Hwang [a,1], Seul-Ki Park [a,b,1], Ha Yeon Lee [a], Seong Who Kim [c], Jung Shin Lee [d,e], Eun Kyung Choi [d,f,g], Dalsan You [h], Choung-Soo Kim [h,*], Nayoung Suh [a,b,*]

[a] Asan Institute for Life Sciences, Asan Medical Center, Seoul 138-736, Republic of Korea
[b] Department of Medicine, Asan Medical Center, University of Ulsan College of Medicine, Seoul 138-736, Republic of Korea
[c] Department of Biochemistry and Molecular Biology, Asan Medical Center, University of Ulsan College of Medicine, Seoul 138-736, Republic of Korea
[d] Institute for Innovative Cancer Research, Asan Medical Center, University of Ulsan College of Medicine, Seoul 138-736, Republic of Korea
[e] Department of Internal Medicine, Asan Medical Center, University of Ulsan College of Medicine, Seoul 138-736, Republic of Korea
[f] Department of Radiation Oncology, Asan Medical Center, University of Ulsan College of Medicine, Seoul 138-736, Republic of Korea
[g] Center for Development and Commercialization of Anti-Cancer Therapeutics, Asan Medical Center, University of Ulsan College of Medicine, Seoul 138-736, Republic of Korea
[h] Department of Urology, Asan Medical Center, University of Ulsan College of Medicine, Seoul 138-736, Republic of Korea

ARTICLE INFO

Article history:
Received 4 April 2014
Revised 24 May 2014
Accepted 30 May 2014
Available online 10 June 2014

Edited by Tamas Dalmay

Keywords:
Human mesenchymal stem cells
miR-140-5p
Bone morphogenic protein 2
Differentiation
Osteogenic lineage commitment

ABSTRACT

Human mesenchymal stem cells (hMSCs) have self-renewal and differentiation capabilities but the regulatory mechanisms of MSC fate determination remain poorly understood. Here, we aimed to identify microRNAs enriched in hMSCs that modulate differentiation commitments. Microarray analysis revealed that miR-140-5p is commonly enriched in undifferentiated hMSCs from various tissue sources. Moreover, bioinformatic analysis and luciferase reporter assay validated that miR-140-5p directly represses bone morphogenic protein 2 (BMP2). Furthermore, blocking miR-140-5p in hMSCs increased the expression of BMP signaling components and critical regulators of osteogenic differentiation. We propose that miR-140-5p functionally inhibits osteogenic lineage commitment in undifferentiated hMSCs.

1. Introduction

Human mesenchymal stem cells (hMSCs) are multipotent stromal cells that have a capability for self-renewal and differentiation [1]. Due to their therapeutic effects, MSCs have been the focus of intensive efforts during recent decades aimed at developing stem cell-based therapies for a wide range of human diseases [2]. Despite the advances made since their discovery, the regulatory mechanisms of MSC fate determination remain poorly understood.

MicroRNAs (miRNAs) are ~22-nucleotide small non-coding RNAs that regulate target genes by both translational inhibition and mRNA destabilization [3]. Numerous studies suggest that miRNAs are key players in many, if not most, fundamental cellular processes and their altered expression may underlie diverse human diseases [4].

There is growing evidence for functional roles of miRNAs in hMSCs. For example, subsets of miRNAs have been identified as regulators of osteogenic differentiation [5–10] and adipogenic differentiation [11–13]. Interestingly, more recent genome-wide analyses have identified that miR-146a-5p and miR-335 regulate hMSC cell proliferation and migration [14,15]. However, miRNAs essential for the regulation of stem cell maintenance and differentiation determination have mainly been studied in embryonic stem cells [16,17].

In our current study, we identified miRNAs, namely miR-140 (both miR-140-5p and miR-140-3p), that are enriched in hMSCs from various human tissues, including adipose, bone marrow, and umbilical cord, compared with fibroblasts, which are a more differentiated mesenchymal cell type. We then demonstrated using target prediction and luciferase reporter assays that bone morphogenic protein 2 (BMP2) is a direct target of miR-140-5p. Furthermore, the inhibition of miR-140-5p expression in hMSCs upregulates BMP2 and its receptors including bone morphogenic

* Corresponding authors at: Asan Institute for Life Sciences, Asan Medical Center, 88 Olympic-ro 43-gil, Songpagu, Seoul 138-736, Republic of Korea. Fax: +82 2 3010 6505.
E-mail addresses: cskim@amc.seoul.kr (C.-S. Kim), nysuh@amc.seoul.kr (N. Suh).
[1] These authors equally contributed to this work.

http://dx.doi.org/10.1016/j.febslet.2014.05.048

protein receptor type II (BMPR2) and type 1B (BMPR1B). The expression of Smad5, an intracellular BMP2 coreceptor, also increased. Interestingly, critical regulators of osteogenic differentiation such as runt-related transcription factor 2 (RUNX2), alkaline phosphatase (ALP), osteocalcin (OCN), and osteopontin (OPN) are expressed in undifferentiated hMSCs upon miR-140-5p inhibition. Furthermore, in the ALP staining assay, the ALP level was increased upon miR-140-5p inhibition, indicating the formation of osteoblasts. Taken together, our data indicate that miR-140-5p represses osteogenic lineage commitment in undifferentiated hMSCs at least in part by negatively regulating BMP2-mediated signaling pathway.

2. Materials and methods

2.1. Cell culture

This study was performed with the approval and in accordance with the guidelines of the Institutional Review Board of the Asan Medical Center. hMSCs from various sources were isolated from donors who provided informed consent. hMSCs were harvested and cultured as previously described [18,19] and characterized for cell surface markers. Human skin and lung fibroblasts were obtained from Medipost (Seoul, Korea). All cell lines were cultured in Dulbecco's modified Eagle's medium (Gibco) supplemented with 10% heat-inactivated fetal bovine serum (Gibco), 100 units/ml penicillin, and 100 μg/ml streptomycin (Gibco) in 5% CO_2 in a humidified incubator at 37 °C. All hMSC experiments were performed at passage 3–6. For osteogenic differentiation, cells were cultured using StemPro osteogenesis differentiation kit (Gibco) according to the manufacturer's instructions.

2.2. miRNA microarray and data analysis

miRNA microarray and data analyses were carried out as previously described [20] using Agilent Human microRNA microarray release 16.0 (G4870A; Agilent Technologies) for profiling. Briefly, total RNA was isolated using Trizol (Life Technologies) and 100 ng per sample was hybridized to the microarray. We compared the expression profiles of two different donors per hMSC to that of fibroblasts. miRNA labeling, hybridization, and washing were performed according to the manufacturer's instructions. Global normalization was performed by using all of the data, and differentially expressed miRNAs were then identified by one-way ANOVA ($P < 0.05$). Thirty-six differentially expressed miRNAs were selected for clustering analysis. Unsupervised hierarchical clustering was performed with average linkage and a heat map was generated in MeV (MultiExperiment Viewer, Boston, MA).

2.3. Target prediction and functional analysis

Conserved target genes of miR-140-5p and miR-140-3p were identified using both TargeScan 6.0 and Ingenuity Pathway Analysis (IPA) software (Qiagen). A confidence level filter was applied for the selection of experimentally observed and/or highly predicted targets in IPA software. The selected lists of genes were then used for core analysis including networks, disease functions, biological functions and canonical pathways.

2.4. Quantitative real-time PCR (qRT-PCR) analysis

Total RNA was isolated from cultured cells using either Trizol reagent (Life Technologies) or a miRVana miRNA isolation kit (Life Technologies) according to the manufacturer's protocol. For mRNA amplification, reverse transcriptase reactions were performed with random hexamers and SuperScript III reverse transcriptase (Life Technologies), and quantitative PCR was done on a 7900 Real-Time PCR system using Power SYBR Green PCR master mix (Applied Biosystems). The primers used in the qRT-PCR can be seen in Supplementary Table 1. For qRT-PCR of miRNAs, miRNAs were first reverse transcribed using a miScript II RT kit and their expression was then quantified using a miScript SYBR Green PCR kit (Qiagen) according to the manufacturer's protocol. SNORD68 or RNU6-2 was used as an endogenous normalization control for miRNAs while GAPDH was used as an mRNA control. Each reaction was performed at least in triplicate and repeated in at least three different donor samples.

2.5. Luciferase reporter assays

To construct a luciferase reporter for wild-type *bmp2* 3′ UTR, we cloned this UTR sequence from the genomic DNA of hMSCs by PCR. PCR products were subcloned into the NotI and XhoI sites in a psiCHECK™-2 vector (Promega). A mutant *bmp2* 3′ UTR was generated by site-directed mutagenesis using Phusion™ High-Fidelity DNA Polymerase (Thermo Scientific) according to the manufacturer's protocol. All constructs were confirmed by sequence analysis. The sequences of the primers are listed in Supplementary Table 2. For transfection, 4×10^4 293T cells were plated in complete medium in a 24-well plate. The next day, the cells were transfected with 50 nM of miR-140-5p mimics or negative control mimics (Thermo Fischer) using Dharmafect1 (Thermo Scientific) following the manufacturer's protocol. Simultaneously, the cells were transfected with luciferase constructs at a concentration of 100 ng per well using FUGENE 6 (Roche) transfection reagent according to the manufacturer's guidelines. Cells were harvested 16 h after transfection in cell lysis buffer and then assayed for luciferase activity using a Dual-Luciferase Reporter Assay System (Promega) on a luminometer following the manufacturer's protocol. Transfection of each construct was performed in triplicate in each assay and the ratios of *Renilla* luciferase readings to firefly luciferase readings were averaged for each experiment.

2.6. Cell transfection

hMSCs were plated at a concentration of 6–7 $\times 10^4$ in complete medium in 6-well plates. The next day, either 50 nM of miRCURYLNA™ Inhibitors (Exiqon) or 10 nM of mimics (Thermo Fischer) were transfected into the cells with DharmaFECT1 (Thermo Scientific) according to the manufacturer's instructions. At 48 h post-transfection, total RNA was isolated using a miRVana miRNA isolation kit (Life Technologies) according to the manufacturer's protocol and used for miRNA and mRNA qRT-PCR analysis.

2.7. Western blotting

Cells were lysed in RIPA buffer (Biosesang) containing Halt™ Protease and Phosphatase Inhibitor Cocktail (Thermo Scientific) at 4 °C. Proteins were separated by 10% SDS–PAGE, transferred to a polyvinylidenedifluoride membrane (Millipore), and probed with anti-BMP2 (Abcam), anti-phospho-SMAD1/5 (Cell signaling), anti-SMAD5 (Cell signaling), anti-BMPR2 (Cell signaling), anti-α-tubulin (Sigma) and anti-GAPDH (Santa Cruz) antibodies. GAPDH or α-tubulin was used as a loading control. Images were obtained on a chemiluminescent image analyzer (LAS-4000 mini; Fujifilm) and quantified by ImageJ software (NIH).

2.8. Alkaline phosphatase (ALP) staining

The formation of osteoblasts was assessed by measuring the levels of ALP staining using Leukocyte Alkaline Phosphatase kit (Sigma). Briefly, hMSCs were plated at a concentration of 1×10^4

in complete medium in 24-well plates. The next day, cells were transfected with either 50 nM of miRCURYLNA™ Inhibitors (Exiqon) or 10 nM of mimics (Thermo Fischer) and incubated for 24 h and then treated with or without 100 ng/ml recombinant human BMP2 (R&D system). In vitro osteogenic differentiation was then carried out using StemPro osteogenesis differentiation kit (Gibco) according to the manufacturer's protocol. At day 7 post osteogenic differentiation, cells were rinsed with cold DPBS and fixed in 4% paraformaldehyde for 30 min at 25 °C. The cell layer was subsequently washed three times with cold DPBS and then once with deionized water. Next, the cells were incubated in FRV-alkaline solution for 20 min at 37 °C and washed with deionized water.

3. Results

3.1. miR-140 is enriched in undifferentiated hMSCs

We hypothesized that the key miRNAs of hMSC required for self-renewal and differentiation fate determination would specifically be found in undifferentiated stem cells rather than in fibroblasts, which are a more differentiated mesenchymal cell type. We therefore compared the genome-wide miRNA expression patterns of undifferentiated human adipose-derived stem cells (ADSCs), bone-marrow-derived stem cells (BMSCs), and umbilical cord-derived stem cells (UCSCs) versus fibroblasts using miRNA microarrays (Fig. 1A and Supplementary Table 3). Among 1347 probes tested, 36 miRNAs showed more than 2-fold differences in their expression levels between at least one hMSC type and fibroblasts ($P < 0.05$). Among these differentially expressed miRNAs, miR-140-5p and miR-140-3p were commonly enriched in all three hMSC types from different tissue sources (Fig. 1B, asterisk in the Venn diagrams). We then validated these microarray results using real-time PCR to monitor the expression of miR-140-5p and miR-140-3p in expanded pools of hMSCs from at least three to nine different donors per sample. Consistent with the array data, both miRNAs were more enriched in all three hMSC types than in fibroblasts (Fig. 1C). Interestingly, cluster analysis using the Euclidean distance of hADSCs, hBMSCs, and hUCSCs showed that the miRNA expression profiles of hADSCs and hBMSCs were more similar to each other than to hUCSCs (Fig. 1D).

3.2. Predictive target genes for miR-140-5p are involved in the intrinsic functions of MSCs

To understand the regulatory functions of miR-140-5p and miR-140-3p, we set out to determine their mRNA targets. A bioinformatic analysis using both TargetScan 6.0 [21] and the Ingenuity Pathway Analysis (IPA, http://www.ingenuity.com/) softwares identified 377 and 114 high confidence target genes for miR-140-5p and miR-140-3p, respectively. We then carried out function and network analysis using these selected target genes. Intriguingly, predicted target genes for both miRNAs showed enrichment of functions related to cellular assembly and organization, cellular function and maintenance and cell morphology. Since target genes for miR-140-5p were more significantly enriched for functions relevant to the proliferation and/or differentiation of MSCs (Table 1), we therefore focused on miR-140-5p in our further investigations.

3.3. miR-140-5p directly represses BMP2 expression in hMSCs

One of the targets of miR-140-5p identified in our screen was BMP2, a potent inducer of osteogenic differentiation. We first monitored the endogenous expression levels of *bmp2* in hMSCs and found that the endogenous *bmp2* transcript levels were significantly downregulated in all types of hMSCs compared with fibroblasts (Fig. 2A). Next, we monitored the expression levels of miR-140-5p during the osteogenic differentiation. Notably, under osteogenic differentiation condition, the miR-140-5-p level was dramatically decreased during the initial steps of differentiation (Fig. 2B, left). Furthermore, the *bmp2* transcript level was drastically increased at day 2 of osteogenic differentiation (Fig. 2B, right),

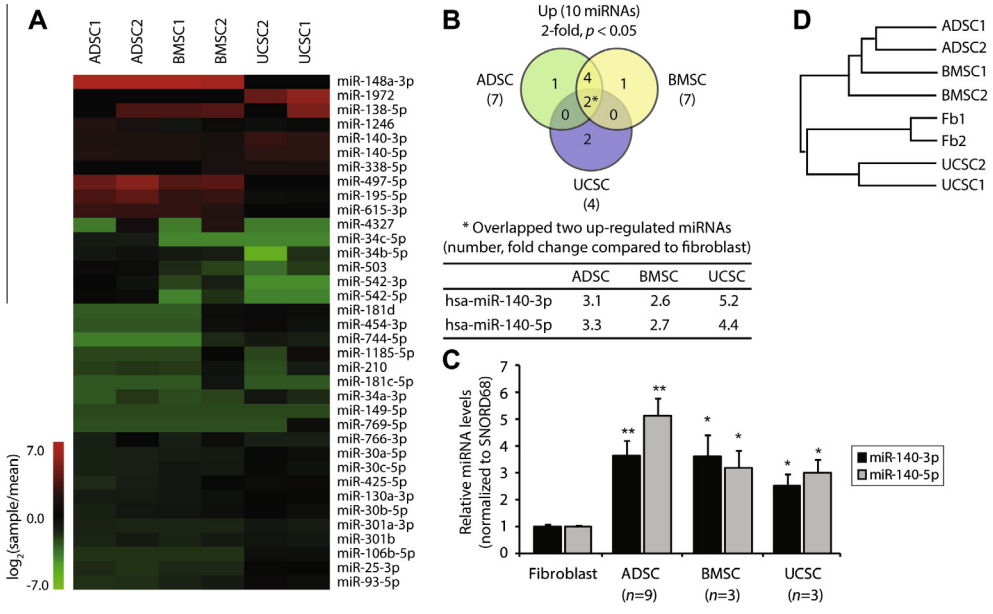

Fig. 1. miR-140 is enriched in undifferentiated hMSCs. (A) Heat map of miRNAs that are enriched in hMSCs compared with human fibroblasts. Red denotes upregulated and green denotes downregulated miRNAs. (B) Venn diagram of the miRNAs differentially expressed in each hMSC from various tissue sources compared with fibroblasts. The asterisk denotes the overlapping of two upregulated miRNAs in all hMSC cell types. The fold changes detected by microarray are denoted in the table. (C) Real-time RT-PCR validation of the miR-140-5p and miR-140-3p expression levels in hMSCs relative to fibroblasts. Error bars denote the standard error of the mean of 10 experiments ($^{*}P < 0.01$; $^{**}P < 0.001$). The number of independent donor samples tested (n) is indicated on the x axis. (D) Dendrogram of the differentially expressed miRNAs of hADSCs, hBMSCs, hUCSCs, and fibroblasts.

Table 1
Principal diseases and molecular and cellular functions associated with the most highly conserved 337 target genes of miR-140-5p (*).

Biological functions	*P* value	No. of molecules
Cellular development	1.19E-07-6.01E-03	114
Differentiation of cells	1.19E-07	80
Proliferation of embryonic cells	4.42E-07	19
Development of osteoblasts	2.28E-06	7
Cellular growth and proliferation	4.42E-07-4.80E-03	120
Proliferation of cells	3.34E-05	118
Proliferation of connective tissue cells	2.60E-04	27
Proliferation of tumor cell lines	1.14E-03	53
Connective tissue development and function	6.00E-09-4.78E-03	66
Abnormal morphology of skull	6.00E-09	21
Differentiation of stromal cells	2.19E-05	6
Mineralization of bone	3.45E-04	10
Embryonic development	6.00E-09-5.52E-03	110
Abnormal morphology of bone	2.13E-07	29
Formation of embryonic tissue	1.35E-06	21
Development of body axis	1.25E-05	42

* These data were generated using IPA software.

the time point when we have observed the most dramatic decrease in the miR-140-5p level. Interestingly, during the later phase of osteogenic differentiation, we observed increased expression levels of miR-140-5p (Supplementary Fig. 1). Considering its well-established roles as a cartilage-specific miRNA, the high levels of miR-140-5p at later osteogenic development were not surprising. Taken together, we concluded that the level of the endogenous miR-140-5p was inversely correlated with that of *bmp2* and tightly regulated during osteogenic differentiation in hMSCs. We speculated that this negative correlation between the endogenous miR-140-5p and *bmp2* levels in hMSCs might be common to all proliferating mesenchymal stem cell types.

Since miRNAs function through their binding to the 3′ untranslated region (UTR) of their target mRNAs [22,23], we constructed a luciferase reporter in which the 3′ UTR of *bmp2* was cloned downstream of the *Renilla* luciferase reporter (Fig. 2C). To confirm that BMP2 is a direct target of miR-140-5p, we cotransfected miR-140-5p mimics with the luciferase reporters in 293T cells. Consistent with the findings of a previous report [24], the overexpression of miR-140-5p inhibited luciferase expression by about 40%, whereas the mock transfection and cotransfection of a negative control mimic had no such inhibitory effect (Fig. 2D, black bars; $P = 0.0043$). Furthermore, a mutation of the miR-140-5p binding sites in the seed sequence significantly diminished this repression, i.e. the luciferase reporter expression was at control levels (Fig. 2D, white bars).

3.4. miR-140-5p inhibition in hMSCs alters the expression of BMP2 and BMP signaling molecules

To determine the functions of miR-140-5p in hMSCs, we transfected these cells with locked nucleic acid (LNA) miRNA inhibitors. Subsequent qRT-PCR analysis revealed a greater than 90% reduction in the miR-140-5p levels (Fig. 3A). Blocking miR-140-5p using LNA-miR-140-5p caused a significant induction of *bmp2* at RNA level, which did not occur upon transfection with a negative control miRNA inhibitor (LNA-NC) (Fig. 3B). Western blot analysis of BMP2 demonstrated that its protein levels were also increased in hMSCs upon inhibition of miR-140-5p expression (Fig. 3C, left). Quantification of these immunoblotting signals from three independent experiments confirmed the upregulation of BMP2 protein levels in LNA-miR-140-5p-treated hMSCs (Fig. 3C, right).

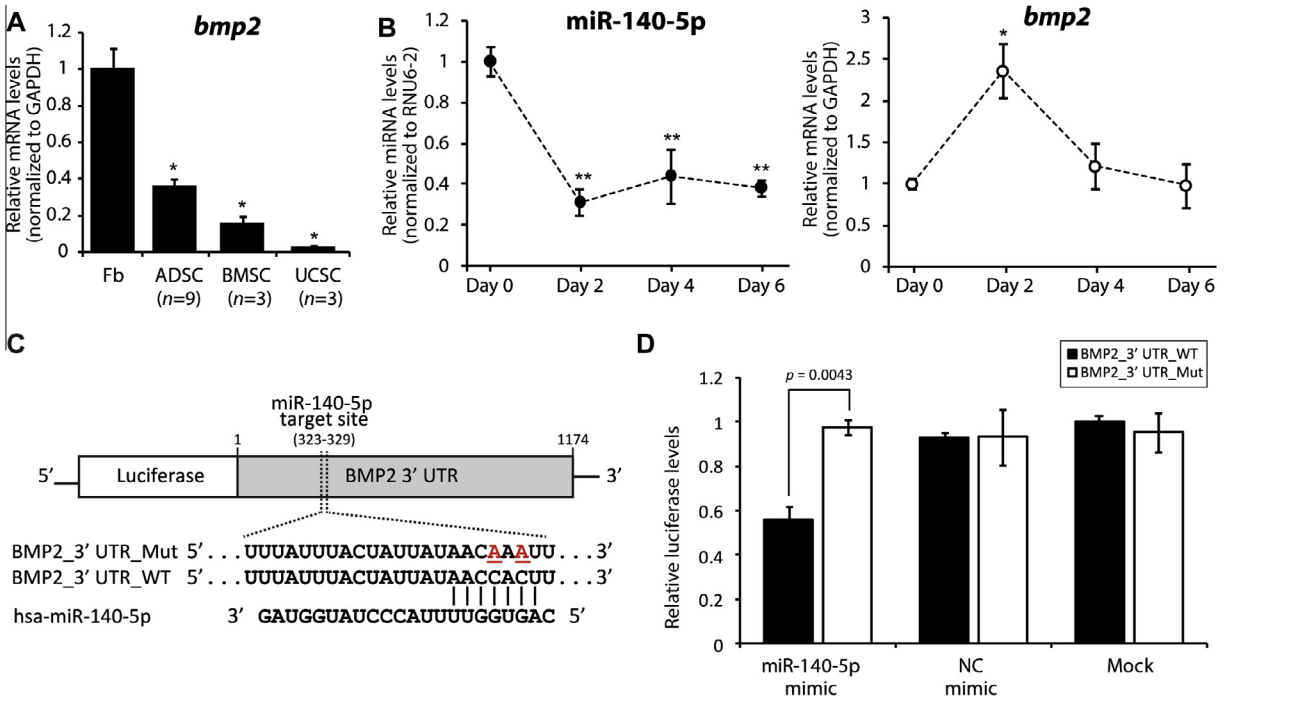

Fig. 2. miR-140-5p directly represses *bmp2* expression. (A) Real-time RT-PCR analysis of *bmp2* transcript levels in undifferentiated hMSCs compared with fibroblasts. Error bars denote the standard error of the mean of 8 experiments (*$P < 0.001$). The number of independent samples tested (n) is indicated on the x axis. (B) Expression levels of miR-140-5p and *bmp2* at indicated time points during the initial steps of osteogenic differentiation. Error bars denote the standard error of the mean of at least 3 independent experiments (*$P < 0.05$; **$P < 0.005$). (C) Schematic of the miR-140-5p target site within the human *bmp2* 3′ UTR and an alignment of miR-140-5p with the wild-type (WT) and mutant (Mut) 3′ UTR regions of *bmp2* showing complementary pairing. The two mutated nucleotides are highlighted in red and underlined. (D) Luciferase reporter assay. 293T cells were cotransfected with luciferase reporters carrying either the wild-type *bmp2* 3′ UTR or the mutated *bmp2* 3′ UTR and 50 nM of a negative control mimic (NC mimic) or miR-140-5p mimic. Error bars denote the standard error of the mean of 3 experiments.

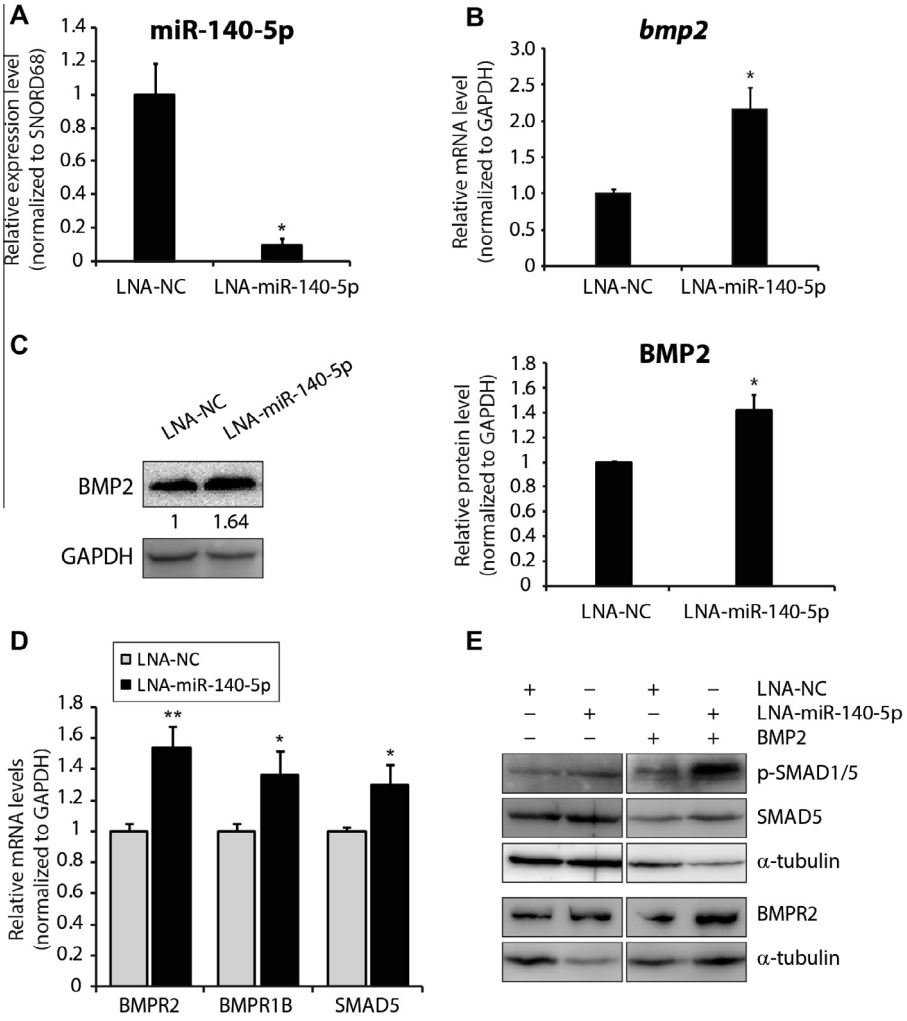

Fig. 3. Inhibition of miR-140-5p alters the expression of BMP2 and BMP signaling molecules in hMSCs. (A) hMSCs were transfected with LNA miR-140-5p inhibitor (50 nM) and RNA was collected 48 h after transfection. qRT-PCR analysis was used to examine the expression of miR-140-5p ($n = 6$) (*$P = 0.0005$). NC, negative control. (B) mRNAs from hMSCs transfected with miR-140-5p inhibitor were analyzed by qRT-PCR ($n = 4$) (*$P = 0.0085$). (C) (Left) Western blot of BMP2 protein in LNA-NC and LNA-miR-140-5p transfected hMSCs. (Right) Quantification of immunoblotted BMP2. To compare replicates, samples were normalized by setting the LNA-negative control (LNA-NC) to a value of 1. Error bars denote the standard error of the mean of 3 experiments (*$P < 0.05$, Student's t-test). (D) qRT-PCR analysis of BMP signaling components. The error bar denotes the standard error of the mean of at least 5 experiments (*$P < 0.05$; **$P < 0.001$). (E) Western blot analysis of phospho-SMAD1/5, SMAD5 and BMPR2. hMSCs were transfected with either LNA-NC or LNA-miR-140-5p for 24 h, then treated with or without BMP2 (100 ng/ml).

The effects of miR-140-5p inhibition on the BMP signaling pathway were next monitored by comparing the transcript levels of key molecules in this pathway. Interestingly, the expression of BMPR2, BMPR1B and SMAD5 significantly increased when miR-140-5p expression was blocked (Fig. 3D). More importantly, the levels of SMAD5, phospho-SMAD1/5 and BMPR2 were enhanced upon miR-140-5p inhibition, and the increases became more significant when hMSCs were treated with BMP2 (Fig. 3E and Supplementary Fig. 2). In contrast, the introduction of the miR-140-5p mimic in hMSCs led to downregulation of SMAD5, phospho-SMAD1/5 and BMPR2 proteins in a BMP2-dependent manner (Supplementary Fig. 3). Taken together, these results suggest that the inhibition of miR-140-5p has a broader impact on BMP signaling in hMSCs.

3.5. Osteogenic markers are abnormally expressed in undifferentiated hMSCs upon miR-140-5p inhibition

To further evaluate the functional activity of miR-140-5p, we monitored the expression patterns of key regulators of osteogenesis after miR-140-5p inhibition under proliferation conditions. After blocking miR-140-5p by LNA inhibitors, the expression levels of osteogenic transcription factors such as RUNX2 and osteogenic markers including ALP, OCN, and OPN were reproducibly increased under proliferation condition (Fig. 4A). Next, we aimed to determine the biological effects of miR-140-5p in osteoblast differentiation by monitoring the expression of ALP. First, we confirmed that the level of miR-140-5p was significantly reduced to more than 69% in LNA-miR-140-5p transfected hMSCs during the osteogenic differentiation (data not shown). Following osteogenic induction, we observed increased levels of ALP staining when miR-140-5p was inhibited (Fig. 4B, top). In addition, ALP staining was enhanced when hMSCs were treated with exogenous BMP2 after inhibiting miR-140-5p (Fig. 4B, bottom). The opposite effects were observed in hMSCs overexpressing miR-140-5p (Supplementary Fig. 4). These results further support the idea that miR-140-5p suppresses BMP2-mediated osteoblast differentiation.

Since the balance between osteogenic and adipogenic differentiation is well-established in hMSCs and its misregulation is often disrupted in various human diseases [25,26], we next examined whether miR-140-5p inhibition would affect adipogenic lineage commitment. Using real-time PCR analysis, we found that the expression level of peroxisome proliferator-activated receptor gamma (*PPARγ*), a key transcription factor in adipogenesis, was expressed similarly in both LNA-NC and LNA-miR-140-5p

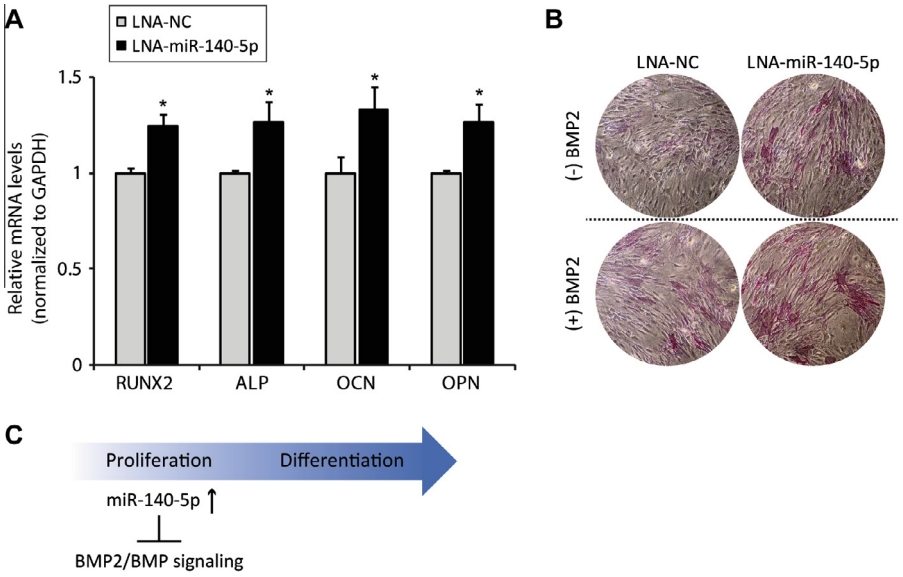

Fig. 4. Key regulators of osteogenesis are misregulated upon miR-140-5p inhibition in hMSCs. (A) Real-time RT-PCR analysis of osteogenic differentiation markers. Error bars denote the standard error of the mean of 3 experiments (*$P < 0.05$). (B) ALP staining at day 7 of osteogenic differentiation showed the increased ALP activity upon miR-140-5p inhibition both in the presence (bottom) and absence (top) of BMP2 (100 ng/ml). (C) A model for the molecular switch controlling osteogenic lineage commitment by miR-140-5p. miR-140-5p functions in undifferentiated hMSCs by suppressing osteogenic differentiation through BMP2 and the BMP signaling pathway. The inhibition of miR-140-5p leads to the misregulation of osteogenic differentiation markers under proliferation state.

transfected hMSCs (Supplementary Fig. 5). Furthermore, adipogenesis markers of differentiation including fatty acid binding protein 4 (*FABP4*) and lipoprotein lipase (*LPL*) were not significantly affected by miR-140-5p inhibition (Supplementary Fig. 5). Hence, we concluded that miR-140-5p has a broad inhibitory effect on osteogenesis in undifferentiated hMSCs.

4. Discussion

The lineage commitments have to be tightly regulated during stem cell maintenance to achieve the fine balance between proliferation and differentiation. Several studies have demonstrated that miRNAs are critical regulators of osteoblast differentiation [27]. We have here identified miR-140-5p as an enriched miRNA in undifferentiated hMSCs which negatively regulates an osteogenic lineage commitment. We also demonstrated that the expression levels of miR-140-5p were dynamically regulated during osteogenic differentiation. Consistent with our findings, recent miRNA profiling studies had demonstrated that miR-140-5p was one of the miRNAs downregulated in various differentiated cell types compared with undifferentiated hMSCs [14,15], but its functional roles had not been investigated in these earlier reports.

Interestingly, cluster analysis of these three groups of hMSCs indicated that ADSCs and BMSCs have more similar miRNA profiles to each other than to UCSCs, reflecting the differences in their origins. Previous studies have demonstrated that even though hMSCs from different tissue sources have a similar morphology and express common surface markers, they show different characteristics in terms of differentiation, proliferation, and motility capability [15,28]. The differences in the miRNA expression profiles of these cell types might underlie these functional diversities.miR-140-5p has long been established as a cartilage-specific miRNA [29] that functions in cartilage homeostasis and osteoarthritis [30,31]. Broader roles for miR-140-5p have only recently been reported. For example, miR-140-5p was previously identified as a potential tumor suppressor in many cancers [32,33] and a circulating miRNA showing a strong correlation with numerous diseases [34–36]. A recent study has also demonstrated that miR-140-5p is involved in testis differentiation in mice [37]. Thus, evidence exists for a diversity of biological functions for miR-140-5p.

In addition to demonstrating the direct repression of BMP2 by miR-140-5p, as previously described [24], we identified its function by inhibiting miR-140-5p expression in hMSCs. We found that miR-140-5p inhibition affected the expression of a subset of BMP signaling components, which are essential for osteoblastic differentiation and bone formation [38]. In addition, we showed that the blocking of miR-140-5p in hMSCs causes an abnormal induction of key regulators of osteogensis in undifferentiated hMSCs. The observed increases in the expression levels upon the miR-140-5p inhibition were not likely due to the direct binding of miR-140-5p to the 3′ UTR regions of the BMP signaling components and osteoblast differentiation markers. An extensive bioinformatic analysis with less stringent miRNA filters using TargestScan 6.0 and IPA softwares revealed the lack of direct binding sites for miR-140-5p in their 3′ UTR regions except for *bmp2* (data not shown). We still note the possibility that miR-140-5p regulates its targets through the region outside of the 3′ UTR. Nevertheless, the increases in their expression upon miR-140-5p inhibition seem to be an indirect consequence of BMP2 induction, which has been observed previously in other systems [8,39]. We therefore suggest that miR-140-5p is a general "stemness" miRNA candidate in undifferentiated hMSCs that modulates the decision of these cells for osteogenic differentiation (Fig. 4C). It remains a challenge to identify the potential roles of miR-140-5p and other likely miRNAs in various lineage commitments that might have a meaningful impact on clinical applications of hMSCs.

5. Accession number

The miRNA profiling data are available at the Gene Expression Omnibus (GEO) database with accession number GSE57266.

Acknowledgements

The authors thank Professor Euiyoung Bae for critical comments on the manuscript. This work was supported by the Basic Science

Research Program through the National Research Foundation of Korea (NRF) funded by the Ministry of Education, Science, and Technology (2012R1A1A3013555), the Next-Generation BioGreen 21 Program (PJ009097) funded by the Rural Development Administration, and the Korean Health Technology R&D Projects funded by Ministry of Health and Welfare, Republic of Korea (A120476 and A121957).

Appendix A. Supplementary data

Supplementary data associated with this article can be found, in the online version, at http://dx.doi.org/10.1016/j.febslet.2014.05.048.

References

[1] Dominici, M., Le Blanc, K., Mueller, I., Slaper-Cortenbach, I., Marini, F., Krause, D., Deans, R., Keating, A., Prockop, D. and Horwitz, E. (2006) Minimal criteria for defining multipotent mesenchymal stromal cells. The International Society for Cellular Therapy position statement. Cytotherapy 8, 315–317.
[2] Bianco, P., Cao, X., Frenette, P.S., Mao, J.J., Robey, P.G., Simmons, P.J. and Wang, C.Y. (2013) The meaning, the sense and the significance: translating the science of mesenchymal stem cells into medicine. Nat. Med. 19, 35–42.
[3] Fabian, M.R. and Sonenberg, N. (2012) The mechanics of miRNA-mediated gene silencing: a look under the hood of miRISC. Nat. Struct. Mol. Biol. 19, 586–593.
[4] Suh, N. and Blelloch, R. (2011) Small RNAs in early mammalian development: from gametes to gastrulation. Development 138, 1653–1661.
[5] Hu, R., Liu, W., Li, H., Yang, L., Chen, C., Xia, Z.Y., Guo, L.J., Xie, H., Zhou, H.D., Wu, X.P. and Luo, X.H. (2011) A Runx2/miR-3960/miR-2861 regulatory feedback loop during mouse osteoblast differentiation. J. Biol. Chem. 286, 12328–12339.
[6] Itoh, T., Nozawa, Y. and Akao, Y. (2009) MicroRNA-141 and -200a are involved in bone morphogenetic protein-2-induced mouse pre-osteoblast differentiation by targeting distal-less homeobox 5. J. Biol. Chem. 284, 19272–19279.
[7] Kim, Y.J., Bae, S.W., Yu, S.S., Bae, Y.C. and Jung, J.S. (2009) MiR-196a regulates proliferation and osteogenic differentiation in mesenchymal stem cells derived from human adipose tissue. J. Bone Miner. Res. 24, 816–825.
[8] Li, Z., Hassan, M.Q., Volinia, S., van Wijnen, A.J., Stein, J.L., Croce, C.M., Lian, J.B. and Stein, G.S. (2008) A microRNA signature for a BMP2-induced osteoblast lineage commitment program. Proc. Natl. Acad. Sci. U.S.A. 105, 13906–13911.
[9] Luzi, E., Marini, F., Sala, S.C., Tognarini, I., Galli, G. and Brandi, M.L. (2008) Osteogenic differentiation of human adipose tissue-derived stem cells is modulated by the miR-26a targeting of the SMAD1 transcription factor. J. Bone Miner. Res. 23, 287–295.
[10] Zeng, Y., Qu, X., Li, H., Huang, S., Wang, S., Xu, Q., Lin, R., Han, Q., Li, J. and Zhao, R.C. (2012) MicroRNA-100 regulates osteogenic differentiation of human adipose-derived mesenchymal stem cells by targeting BMPR2. FEBS Lett. 586, 2375–2381.
[11] Sun, F., Wang, J., Pan, Q., Yu, Y., Zhang, Y., Wan, Y., Wang, J., Li, X. and Hong, A. (2009) Characterization of function and regulation of miR-24-1 and miR-31. Biochem. Biophys. Res. Commun. 380, 660–665.
[12] Yang, Z., Bian, C., Zhou, H., Huang, S., Wang, S., Liao, L. and Zhao, R.C. (2011) MicroRNA hsa-miR-138 inhibits adipogenic differentiation of human adipose tissue-derived mesenchymal stem cells through adenovirus EID-1. Stem Cells Dev. 20, 259–267.
[13] Esau, C., Kang, X., Peralta, E., Hanson, E., Marcusson, E.G., Ravichandran, L.V., Sun, Y., Koo, S., Perera, R.J., Jain, R., Dean, N.M., Freier, S.M., Bennett, C.F., Lollo, B. and Griffey, R. (2004) MicroRNA-143 regulates adipocyte differentiation. J. Biol. Chem. 279, 52361–52365.
[14] Tome, M., Lopez-Romero, P., Albo, C., Sepulveda, J.C., Fernandez-Gutierrez, B., Dopazo, A., Bernad, A. and Gonzalez, M.A. (2011) MiR-335 orchestrates cell proliferation, migration and differentiation in human mesenchymal stem cells. Cell Death Differ. 18, 985–995.
[15] Hsieh, J.Y., Huang, T.S., Cheng, S.M., Lin, W.S., Tsai, T.N., Lee, O.K. and Wang, H.W. (2013) MiR-146a-5p circuitry uncouples cell proliferation and migration, but not differentiation, in human mesenchymal stem cells. Nucleic Acids Res. 41, 9753–9763.
[16] Wang, Y., Baskerville, S., Shenoy, A., Babiarz, J.E., Baehner, L. and Blelloch, R. (2008) Embryonic stem cell-specific microRNAs regulate the G1-S transition and promote rapid proliferation. Nat. Genet. 40, 1478–1483.
[17] Wang, Y., Medvid, R., Melton, C., Jaenisch, R. and Blelloch, R. (2007) DGCR8 is essential for microRNA biogenesis and silencing of embryonic stem cell self-renewal. Nat. Genet. 39, 380–385.
[18] Zuk, P.A., Zhu, M., Mizuno, H., Huang, J., Futrell, J.W., Katz, A.J., Benhaim, P., Lorenz, H.P. and Hedrick, M.H. (2001) Multilineage cells from human adipose tissue: implications for cell-based therapies. Tissue Eng. 7, 211–228.
[19] Zuk, P.A., Zhu, M., Ashjian, P., De Ugarte, D.A., Huang, J.I., Mizuno, H., Alfonso, Z.C., Fraser, J.K., Benhaim, P. and Hedrick, M.H. (2002) Human adipose tissue is a source of multipotent stem cells. Mol. Biol. Cell 13, 4279–4295.
[20] Kim, N., Kim, H., Jung, I., Kim, Y., Kim, D. and Han, Y.M. (2011) Expression profiles of miRNAs in human embryonic stem cells during hepatocyte differentiation. Hepatol. Res. 41, 170–183.
[21] Lewis, B.P., Shih, I.H., Jones-Rhoades, M.W., Bartel, D.P. and Burge, C.B. (2003) Prediction of mammalian microRNA targets. Cell 115, 787–798.
[22] Ambros, V. (2001) MicroRNAs: tiny regulators with great potential. Cell 107, 823–826.
[23] Bartel, D.P. (2004) MicroRNAs: genomics, biogenesis, mechanism, and function. Cell 116, 281–297.
[24] Nicolas, F.E., Pais, H., Schwach, F., Lindow, M., Kauppinen, S., Moulton, V. and Dalmay, T. (2011) MRNA expression profiling reveals conserved and non-conserved miR-140 targets. RNA Biol. 8, 607–615.
[25] Kajkenova, O., Lecka-Czernik, B., Gubrij, I., Hauser, S.P., Takahashi, K., Parfitt, A.M., Jilka, R.L., Manolagas, S.C. and Lipschitz, D.A. (1997) Increased adipogenesis and myelopoiesis in the bone marrow of SAMP6, a murine model of defective osteoblastogenesis and low turnover osteopenia. J. Bone Miner. Res. 12, 1772–1779.
[26] Kaplan, F.S. and Shore, E.M. (2000) Progressive osseous heteroplasia. J. Bone Miner. Res. 15, 2084–2094.
[27] Taipaleenmaki, H., Bjerre Hokland, L., Chen, L., Kauppinen, S. and Kassem, M. (2012) Mechanisms in endocrinology: micro-RNAs: targets for enhancing osteoblast differentiation and bone formation. Eur. J. Endocrinol. 166, 359–371.
[28] Hsieh, J.Y., Fu, Y.S., Chang, S.J., Tsuang, Y.H. and Wang, H.W. (2010) Functional module analysis reveals differential osteogenic and stemness potentials in human mesenchymal stem cells from bone marrow and Wharton's jelly of umbilical cord. Stem Cells Dev. 19, 1895–1910.
[29] Miyaki, S., Sato, T., Inoue, A., Otsuki, S., Ito, Y., Yokoyama, S., Kato, Y., Takemoto, F., Nakasa, T., Yamashita, S., Takada, S., Lotz, M.K., Ueno-Kudo, H. and Asahara, H. (2010) MicroRNA-140 plays dual roles in both cartilage development and homeostasis. Genes Dev. 24, 1173–1185.
[30] Swingler, T.E., Wheeler, G., Carmont, V., Elliott, H.R., Barter, M.J., Abu-Elmagd, M., Donell, S.T., Boot-Handford, R.P., Hajihosseini, M.K., Munsterberg, A., Dalmay, T., Young, D.A. and Clark, I.M. (2012) The expression and function of microRNAs in chondrogenesis and osteoarthritis. Arthritis Rheum. 64, 1909–1919.
[31] Karlsen, T.A., Jakobsen, R.B., Mikkelsen, T.S. and Brinchmann, J.E. (2014) MicroRNA-140 targets RALA and regulates chondrogenic differentiation of human mesenchymal stem cells by translational enhancement of SOX9 and ACAN. Stem Cells Dev. 23, 290–304.
[32] Yang, H., Fang, F., Chang, R. and Yang, L. (2013) MicroRNA-140-5p suppresses tumor growth and metastasis by targeting transforming growth factor beta receptor 1 and fibroblast growth factor 9 in hepatocellular carcinoma. Hepatology 58, 205–217.
[33] Mosakhani, N., Lahti, L., Borze, I., Karjalainen-Lindsberg, M.L., Sundstrom, J., Ristamaki, R., Osterlund, P., Knuutila, S. and Sarhadi, V.K. (2012) MicroRNA profiling predicts survival in anti-EGFR treated chemorefractory metastatic colorectal cancer patients with wild-type KRAS and BRAF. Cancer Genet. 205, 545–551.
[34] Ortega, F.J., Mercader, J.M., Catalan, V., Moreno-Navarrete, J.M., Pueyo, N., Sabater, M., Gomez-Ambrosi, J., Anglada, R., Fernandez-Formoso, J.A., Ricart, W., Fruhbeck, G. and Fernandez-Real, J.M. (2013) Targeting the circulating microRNA signature of obesity. Clin. Chem. 59, 781–792.
[35] Ortega, F.J., Mercader, J.M., Moreno-Navarrete, J.M., Rovira, O., Guerra, E., Esteve, E., Xifra, G., Martinez, C., Ricart, W., Rieusset, J., Rome, S., Karczewska-Kupczewska, M., Straczkowski, M. and Fernandez-Real, J.M. (2014) Profiling of circulating micrornas reveals common microRNAs linked to type 2 diabetes that change with insulin sensitization. Diabetes Care.
[36] Cui, L., Qi, Y., Li, H., Ge, Y., Zhao, K., Qi, X., Guo, X., Shi, Z., Zhou, M., Zhu, B., Guo, Y., Li, J., Stratton, C.W., Tang, Y.W. and Wang, H. (2011) Serum microRNA expression profile distinguishes enterovirus 71 and coxsackievirus 16 infections in patients with hand-foot-and-mouth disease. PLoS One 6, e27071.
[37] Rakoczy, J., Fernandez-Valverde, S.L., Glazov, E.A., Wainwright, E.N., Sato, T., Takada, S., Combes, A.N., Korbie, D.J., Miller, D., Grimmond, S.M., Little, M.H., Asahara, H., Mattick, J.S., Taft, R.J. and Wilhelm, D. (2013) MicroRNAs-140-5p/140-3p modulate Leydig cell numbers in the developing mouse testis. Biol. Reprod. 88, 143.
[38] Chen, G., Deng, C. and Li, Y.P. (2012) TGF-beta and BMP signaling in osteoblast differentiation and bone formation. Int. J. Biol. Sci. 8, 272–288.
[39] Katagiri, T., Yamaguchi, A., Komaki, M., Abe, E., Takahashi, N., Ikeda, T., Rosen, V., Wozney, J.M., Fujisawa-Sehara, A. and Suda, T. (1994) Bone morphogenetic protein-2 converts the differentiation pathway of C2C12 myoblasts into the osteoblast lineage. J. Cell Biol. 127, 1755–1766.